

## ***Supplementary Materials***

# **A superior lithium-ion capacitor based on ultrafine MnO/dual N-doped carbon anode and porous carbon cathode**

*Da Lei<sup>1</sup>, †, Yuyang Gao<sup>1</sup>, †, Zhidong Hou<sup>1</sup>, Lingbo Ren<sup>1</sup>, Mingwei Jiang<sup>1</sup>, Yunjing Cao<sup>1</sup>, Yu Zhang<sup>2</sup>,\*, Jian-Gan Wang<sup>1,\*</sup>*

<sup>1</sup> State Key Laboratory of Solidification Processing, Shaanxi Joint Lab of Graphene, School of Materials Science and Engineering, Northwestern Polytechnical University, No. 127, Youyi West Road, Xi'an 710072, China

<sup>2</sup> School of Mechanical and Power Engineering, East China University of Science and Technology, 130 Meilong Road, Shanghai 200237, China

\* Correspondence: wangjiangan@nwpu.edu.cn (J.-G. Wang); yzhang071@ecust.edu.cn (Y. Zhang)

† These authors contributed equally to this work

## Supplementary Figures and Tables

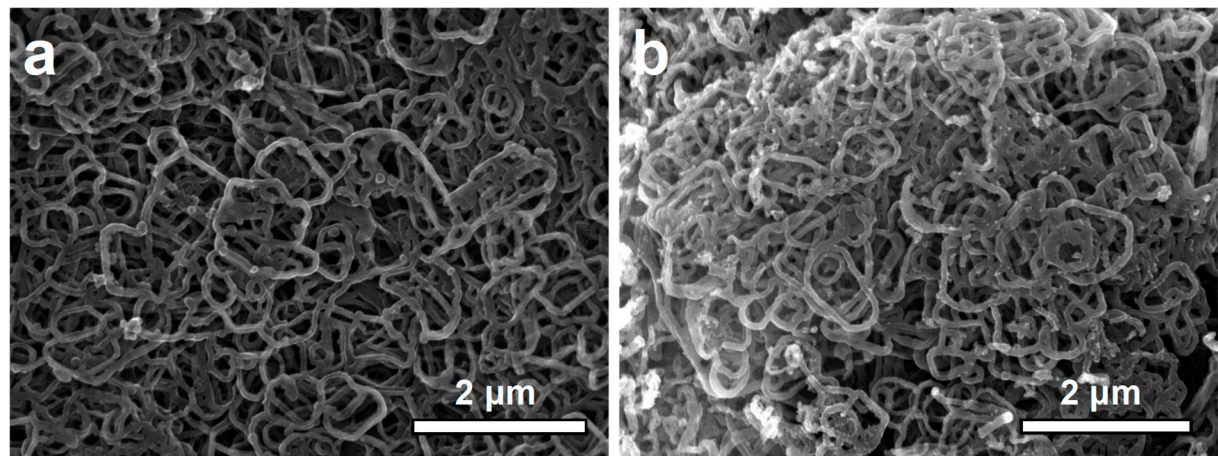


**Figure S1.** SEM images of (a) PPy and (b) MnO/DNC at different magnification.

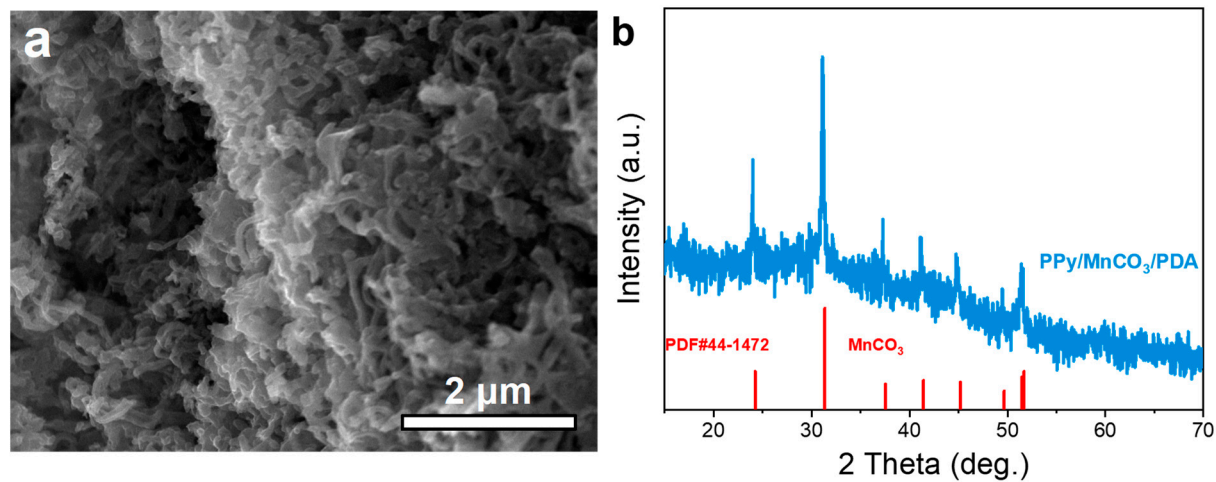


**Figure S2.** (a) SEM image and (b) XRD pattern of PPy/MnCO<sub>3</sub>/PDA.

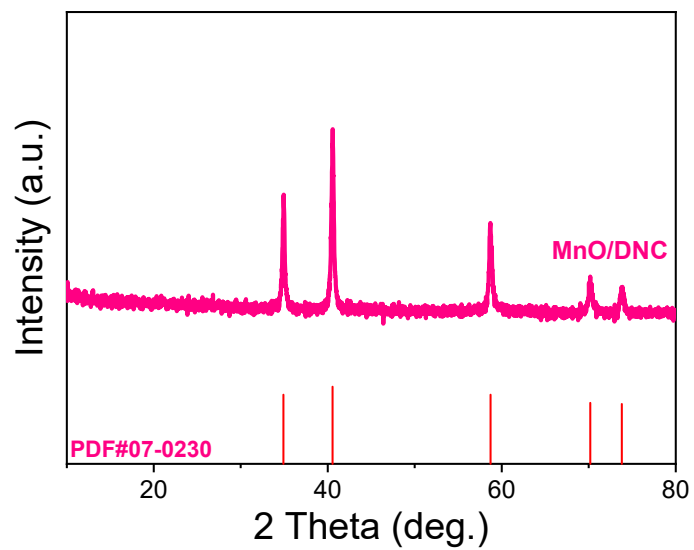


**Figure S3.** XRD pattern of MnO/DNC.

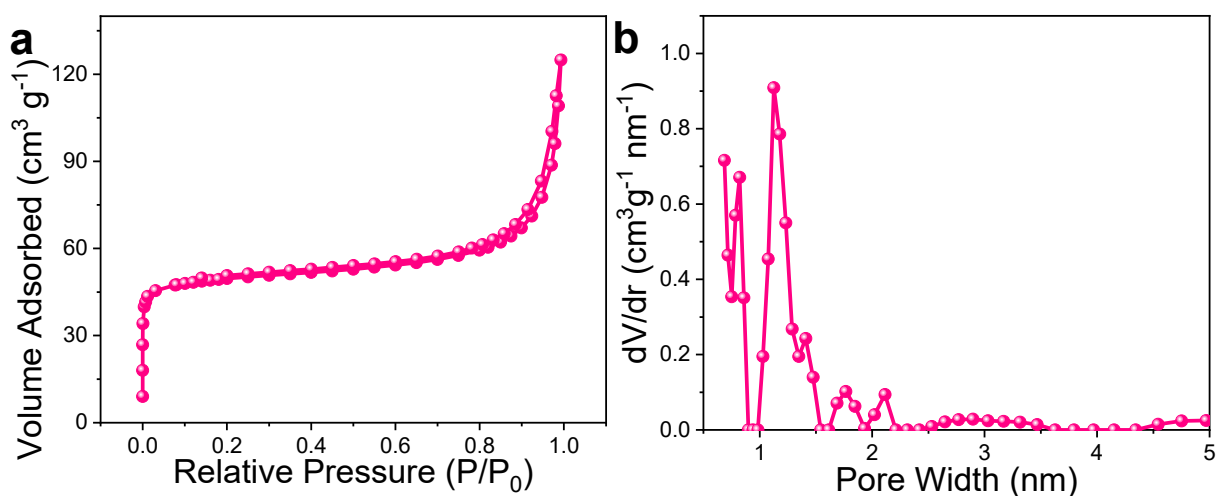


**Figure S4.** (a) BET curve and (b) the corresponding pore-size distribution of MnO/DNC.

**Table S1.** The comparison of present work with other reported MnO-based anodes.

Sample	Rate performance	Current density ( $\text{A g}^{-1}$ )	Cycle number	Capacity retention ( $\text{mAh g}^{-1}$ )	Ref.
MnO/DNC	406 $\text{mAh g}^{-1}$ (@2 $\text{A g}^{-1}$ ) /179 $\text{mAh g}^{-1}$ (@10 $\text{A g}^{-1}$ )	0.1/2	100/500	682(95%) /393(97%)	This work
MnO/C aerogel	601 $\text{mAh g}^{-1}$ (@2 $\text{A g}^{-1}$ )	0.2	140	1177(150%)	[S1]
MnO@C nanoplates	770 $\text{mAh g}^{-1}$ (@0.2 $\text{A g}^{-1}$ )	0.2	30	563(73%)	[S2]
MnO@C microspheres	238 $\text{mAh g}^{-1}$ (@0.8 $\text{A g}^{-1}$ )	0.1	100	525(82%)	[S3]
MnO/NC nanorods	49 $\text{mAh g}^{-1}$ (@5 $\text{A g}^{-1}$ )	1	600	570	[S4]
MnO-Cu-CNT /graphene	432 $\text{mAh g}^{-1}$ (@3.2 $\text{A g}^{-1}$ )	0.1	50	857(110%)	[S5]
Fusiform MnO particles	203 $\text{mAh g}^{-1}$ (@2 $\text{A g}^{-1}$ )	0.1	100	747	[S6]
MnO/C nanowires	315 $\text{mAh g}^{-1}$ (@2 $\text{A g}^{-1}$ )	1	600	480	[S7]
MnO@C nanofibers	328 $\text{mAh g}^{-1}$ (@4 $\text{A g}^{-1}$ )	0.5	200	156%	[S8]

**Table S2.** Fitted impedance parameters and equivalent circuit.

<b>Sample</b>	<b><math>R_s</math> (<math>\Omega</math>)</b>	<b><math>R_{ct}</math> (<math>\Omega</math>)</b>
NC	0.7	51.2
MnO/DNC	1.9	71.6

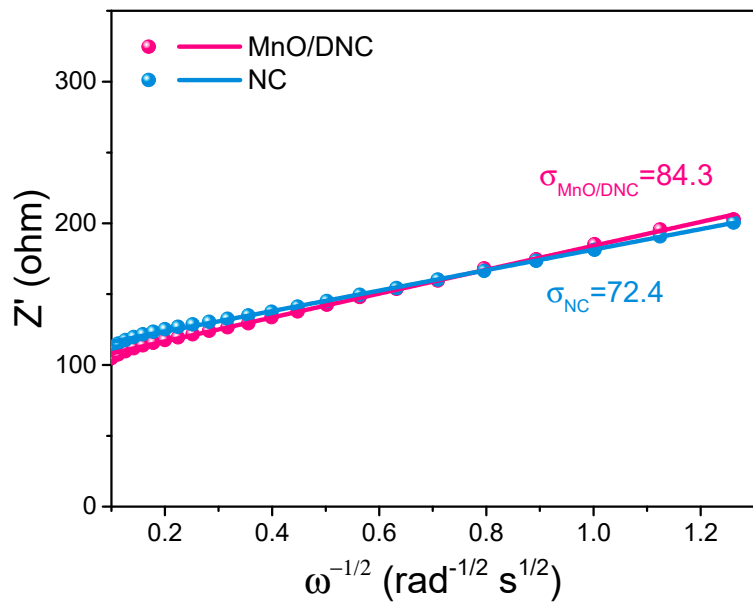


**Figure S5.** The linear relationship between  $Z'$  and the  $\omega^{-1/2}$  of NC and MnO/DNC.

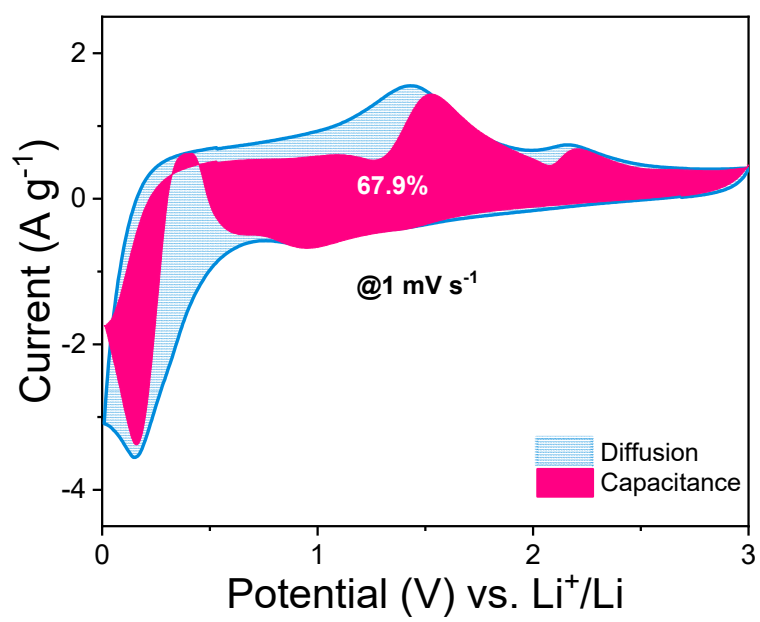


**Figure S6.** Capacitive contribution (pink region) of the MnO/DNC electrode at  $1 \text{ mV s}^{-1}$ .

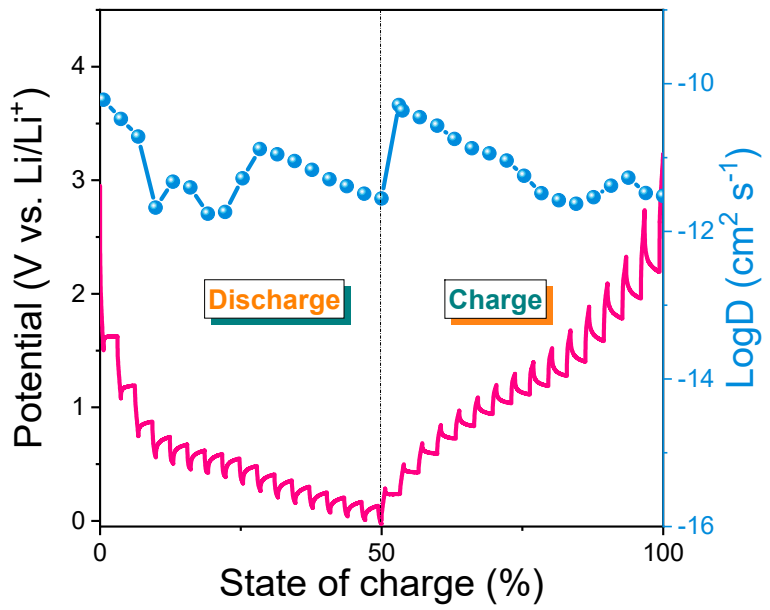


**Figure S7.** GITT curve and calculated  $D_{Li^+}$  of MnO/DNC.

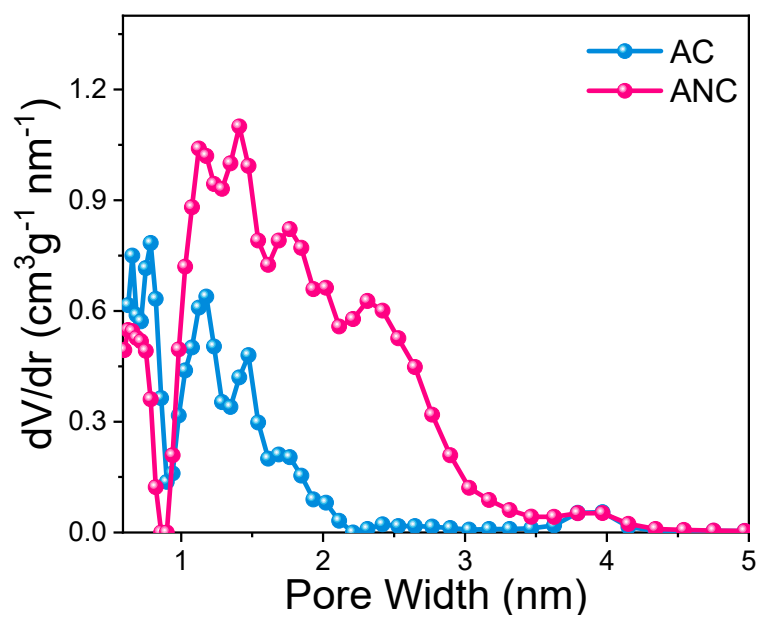


**Figure S8.** The corresponding pore-size distribution of AC and ANC.

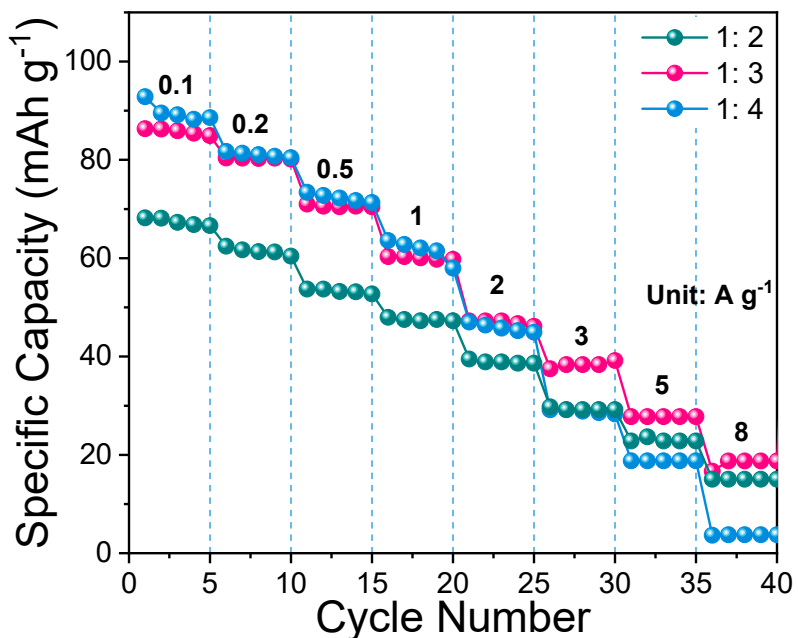


**Figure S9.** Rate capabilities of MnO/DNC//ANC LICs with different mass ratios

## Reference

- [S1] Liu, R.; Chen, X.; Zhou, C.; Li, A.; Gong, Y.; Muhammad, N.; Song, H. Controlled synthesis of porous 3D interconnected MnO/C composite aerogel and their excellent lithium-storage properties. *Electrochim. Acta* **2019**, *306*, 143-150, doi:10.1016/j.electacta.2019.03.129.
- [S2] Zhang, X.; Xing, Z.; Wang, L.; Zhu, Y.; Li, Q.; Liang, J.; Yu, Y.; Huang, T.; Tang, K.; Qian, Y.; et al. Synthesis of MnO@C core–shell nanoplates with controllable shell thickness and their electrochemical performance for lithium-ion batteries. *Journal of Materials Chemistry* **2012**, *22*, 17864, doi:10.1039/c2jm32421k.
- [S3] Guo, S.; Lu, G.; Qiu, S.; Liu, J.; Wang, X.; He, C.; Wei, H.; Yan, X.; Guo, Z. Carbon-coated MnO microparticulate porous nanocomposites serving as anode materials with enhanced electrochemical performances. *Nano Energy* **2014**, *9*, 41-49, doi:10.1016/j.nanoen.2014.06.025.
- [S4] Wang, Y.; Chen, X.; Liu, Z.; Wu, H.; Zhao, H.; Liu, H.; Zhang, Y. Cycling-induced structure refinement of MnO nanorods wrapped by N-doped carbon with internal void space for advanced lithium-ion anodes. *Appl. Surf. Sci.* **2019**, *479*, 386-394, doi:10.1016/j.apsusc.2019.02.144.
- [S5] Wang, J.; Deng, Q.; Li, M.; Jiang, K.; Hu, Z.; Chu, J. High-capacity and long-life lithium storage boosted by pseudocapacitance in three-dimensional MnO-Cu-CNT/graphene anodes. *Nanoscale* **2018**, *10*, 2944-2954, doi:10.1039/c7nr08191j.

- [S6] Pei, X.; Mo, D.; Lyu, S.; Zhang, J.; Fu, Y. Preparation of novel two-stage structure MnO micrometer particles as lithium-ion battery anode materials. *RSC Adv.* **2018**, *8*, 28518-28524, doi:10.1039/c8ra03051k.
- [S7] Wang, J.; Zhang, C.; Jin, D.; Xie, K.; Wei, B. Synthesis of ultralong MnO/C coaxial nanowires as freestanding anodes for high-performance lithium ion batteries. *J. Mater. Chem. A* **2015**, *3*, 13699-13705, doi:10.1039/c5ta02440d.
- [S8] Chen, Z.; He, B.; Yan, D.; Yu, X.; Li, W. Peapod-like MnO@hollow carbon nanofibers film as self-standing electrode for Li-ion capacitors with enhanced rate capacity. *J. Power Sources* **2020**, *472*, 228501, doi:10.1016/j.jpowsour.2020.228501.